AIAA JOURNAL
Vol. 32, No. 2, February 1994

Unsteady Flow Phenomena over Delta Wings at High Angle of Attack

Ismet Gursul*
University of Cincinnati, Cincinnati, Ohio 45221

Experiments show that coherent pressure fluctuations observed on delta wings are due to the helical mode instability of the vortex breakdown flowfield. No dominant frequency in the spectra of pressure fluctuations on the wing surface was observed after the breakdown reached the apex of the wing, although the vortex shedding could be detected in the wake. Measurements of pressure fluctuations at different streamwise locations on the wing suggest that the dimensionless frequency fx/U_∞ is nearly constant for a given geometry, which implies increasing wavelength in the streamwise direction. For different wings, this nondimensional frequency is shown to be a function of nondimensional circulation $\Gamma/U_\infty x$ only. Both the wavelength of the disturbances and the core radius increase with the nondimensional circulation at a fixed streamwise location. The wavelength normalized by the core radius is around 3–4, which is much smaller than the predictions for the Q vortex.

Nomenclature

c = root chord
f = frequency
k = axial wave number
n = azimuthal wave number
p = pressure
q = parameter for Q vortex
Re = Reynolds number
r = radial distance from vortex axis
r_0 = characteristic core size
s = local semispan
U_∞ = freestream velocity
U_c = phase speed
U_s = axial velocity excess or deficit
V = azimuthal velocity
W = axial velocity
x = chordwise distance from wing apex
y = spanwise distance from wing root
z = distance above wing surface
α = angle of attack
Γ = leading-edge vortex circulation
θ = phase angle
Λ = sweep angle
λ = wavelength
ρ = density
Φ = phase angle
ϕ = azimuthal angle
ω = radial frequency

Introduction

ALTHOUGH interest in high angle-of-attack aerodynamics has increased, little is known about unsteady flow in vortex breakdown/postbreakdown flowfields. Sharply increased fluctuations in the normal-force coefficient for delta wings were observed when vortex breakdown moved over the wing.[1] Measurements of surface pressure fluctuations in the wake of breakdown showed coherent oscillations.[2,3] Periodic oscillations were also observed in other swirling flows after breakdown occurred.[4–7] Garg and Leibovich carried out LDV measurements in the wakes of breakdown in tubes and observed coherent oscillations. They suggested that the measured frequencies correspond to the theoretical predictions found in Ref. 8 for the first helical mode ($n = -1$) of the time-averaged mean flow profiles, assuming that the oscillations are the disturbances with the maximum growth rate. [The disturbances are represented as $\exp\{i(kx + n\phi - \omega t)\}$, where ω is the frequency, k the wave number in the axial direction, and n the wave number (an integer) in the angular direction]. Thus, one possible source of the observed oscillations over delta wings is the hydrodynamic instability of breakdown wake.

On the other hand, based on the velocity measurements in the wake of a delta wing, vortex shedding was shown to occur.[9] It was suggested that the alternate shedding at large angle of attack should induce asymmetry on the pressure distribution on the wing. The smallest angle of attack for which the periodic motion was detected was around 35 deg for the particular delta wing used. Although the authors do not report the location of vortex breakdown, it is estimated to be over the wing and close to the trailing edge.[10,11] This suggests that vortex shedding may start when the breakdown moves over the wing. Although the time-averaged velocity measurements (for example, see Hummel[12]) reveal that the swirling flow persists in the wake of breakdown, little is known about the instantaneous flow structure. Since the axial convection of vorticity along the core is reduced after the breakdown, vortex shedding might start from the wing.

The purpose of this study is to investigate the characteristics of unsteady flow over delta wings of different sweep angle. The nature of coherent oscillations, their origin (helical mode instability vs vortex shedding), and their influence on unsteady loading will be discussed with the aid of measurements of pressure and velocity as well as flow visualization.

Experimental Setup

The experiments were carried out in an open-circuit wind tunnel having a cross section of 305 mm × 305 mm. The flow entered through a 9.5:1 contraction section with honeycomb and screens, passed through the test section, and was exhausted by an axial fan. The turbulence intensity in the test section was about 0.25%. The freestream velocity spectrum was free from any sharp peaks. The angle of attack of the wings could be varied continuously from outside the tunnel.

Pressure and velocity measurements were made for four delta wings with sweep angles Λ = 60, 65, 70, and 75 deg. The chord lengths ranged from 120 mm to 150 mm, and the models were constructed of 9.5-mm-thick PVC. The lee surfaces were flat whereas the leading edges were beveled at 45 deg on the windward side. The models were sting mounted. The measurements were done at Reynolds numbers based on the chord length equal to 25,000–

Received Dec. 16, 1992; revision received June 1, 1993; accepted for publication June 2, 1993.

*Assistant Professor, Department of Mechanical, Industrial, and Nuclear Engineering.

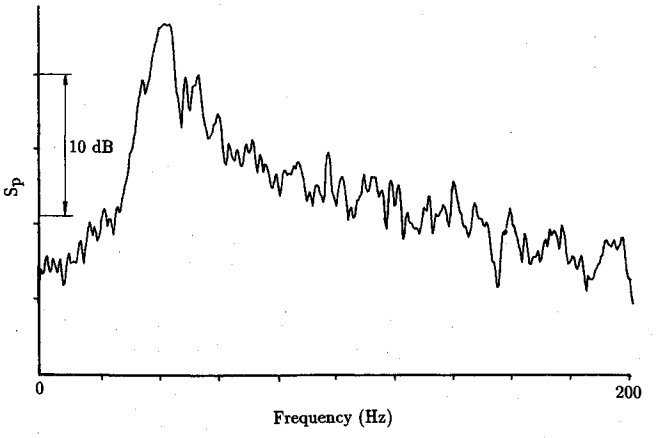

Fig. 1 Spectrum of pressure fluctuations at $x/c = 0.89$, $y/s = 0.42$, $\alpha = 35.3$ deg, $\Lambda = 70$ deg; vertical scale is logarithmic.

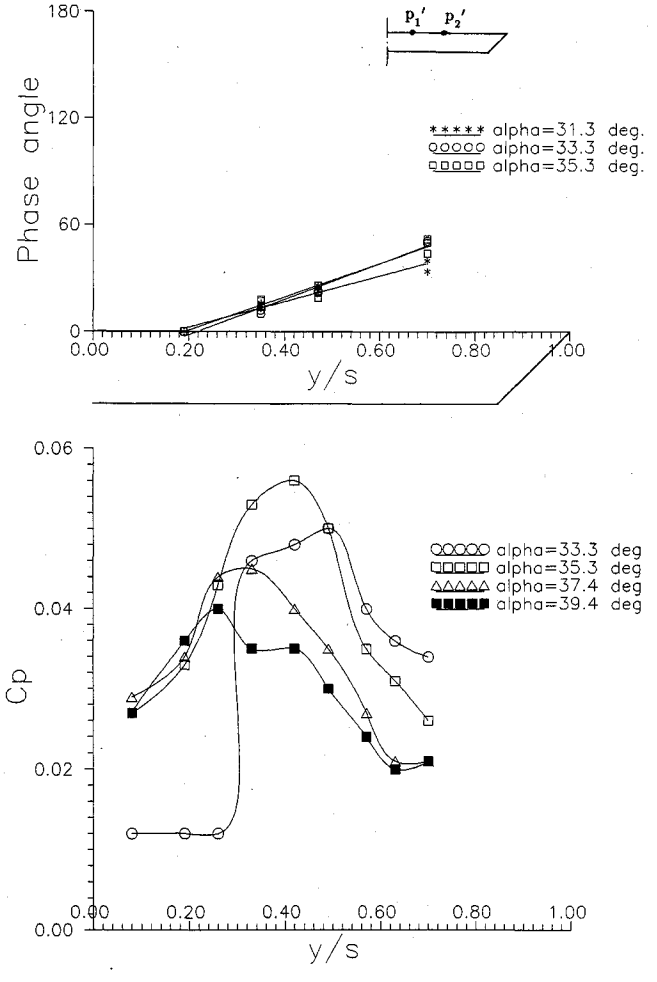

Fig. 2 Phase delay between the pressure fluctuations measured at points 1 and 2; point 1 is fixed, while the location of point 2 is varied (top). Variation of the amplitude of pressure fluctuations (bottom), $\Lambda = 70$ deg.

100,000, although most of the results reported here correspond to $Re \simeq 100{,}000$. At the largest angle of attack, the blockage ratio was 0.094. A piezoelectric pressure transducer (PCB, model 103A) was used to measure the fluctuating pressure on the wing surface. The transducer has been flush mounted at the surface. The transducer and its leads were housed in the grooves running either along a ray from the apex to the trailing edge (at 40–60% of the local semispan, depending on the sweep angle) or along the spanwise direction. The pressure sensing part of the transducers had a diameter of 2.54 mm. Two pressure transducers were used for simultaneous measurements in the spanwise and streamwise directions. A hot-wire probe was used to obtain the spectra of the velocity fluctuations over the wing and in the wake. Pressure and velocity signals were processed by a two-channel signal analyzer (HP 35660A). Smoke-wire visualization by a 0.1-mm-diam stainless steel wire, and the smoke injected near the apex provided information on the flow structure and vortex breakdown location. A light source consisting of two 600-W lamps was used to illuminate the flowfield. In addition to the still pictures taken, flow visualization was videotaped at low speeds. The measurement uncertainty for dimensionless pressure coefficient ranged from 10% to 0.6%, whereas the uncertainty for frequency and breakdown location were estimated as 1.4% and 3%, respectively.

Results

When the vortex breakdown moved over the wing, the pressure fluctuations exhibited coherent oscillations. An example of pressure fluctuation spectrum for sweep angle $\Lambda = 70$ deg, at an angle of attack $\alpha = 35.3$ deg is shown in Fig. 1. The measurement was taken at $x/c = 0.89$, $y/s = 0.42$ (where s is the local semispan) and the vortex breakdown location was $x_b/c \simeq 0.3$. A sharp peak in the spectra was always observed in the wake of breakdown location, regardless of angle of attack and sweep angle for all of the delta wings tested. In the Reynolds number range investigated, the dimensionless dominant frequency fc/U_∞ seemed to be independent

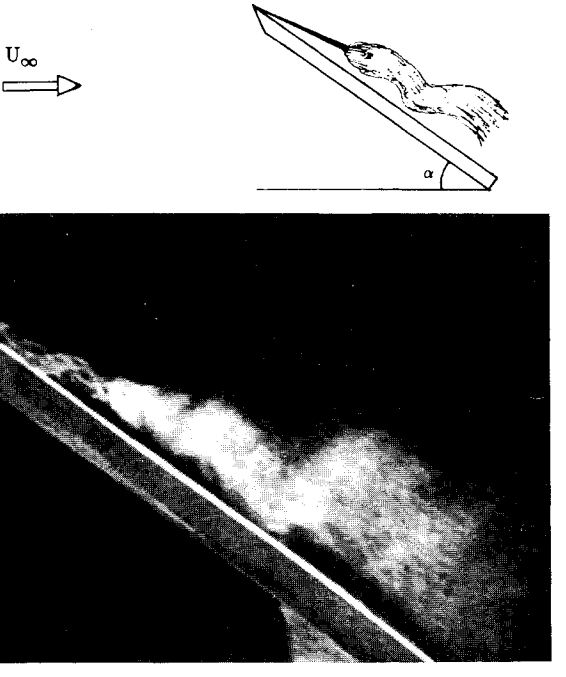

Fig. 3 Smoke visualization showing helical instability in the breakdown region ($\alpha = 35$ deg, $\Lambda = 70$ deg), $Re = 15{,}000$.

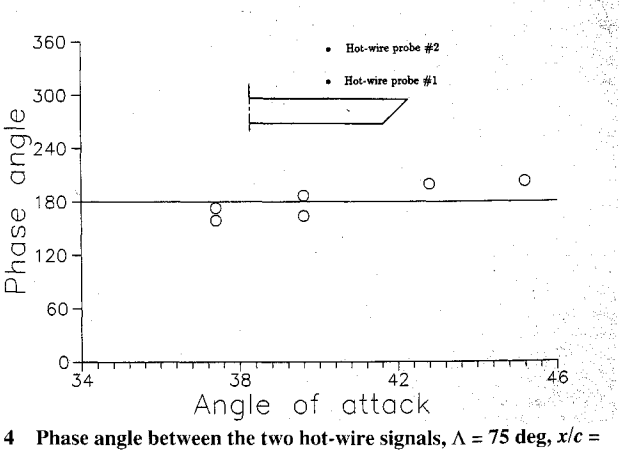

Fig. 4 Phase angle between the two hot-wire signals, $\Lambda = 75$ deg, $x/c = 0.89$.

of the Reynolds number. To understand the nature of these oscillations, measurements were taken with two pressure transducers located in the spanwise direction. Cross-spectral analysis provided the phase angle between the pressure fluctuations measured with the two transducers. If the pressure fluctuations are represented as $\cos(\omega t)$ and $\cos(\omega t - \theta)$ at points 1 and 2, respectively, the phase angle θ is shown in Fig. 2 together with the amplitude ($C_p = p'_{rms}/\frac{1}{2}\rho U_\infty^2$) distribution in the spanwise direction. In measuring the phase angle, the location of point 1 was fixed while the location of point 2 was varied. Increase in phase delay toward the leading edge is consistent with the direction of rotation in the vortex. The vortex shedding from the leading edge cannot cause this variation of the phase delay. Instead, the trend would likely be opposite (i.e., decreasing phase lag toward the leading edge). Thus, the evidence suggests that the oscillations may be due to the helical mode instability. Indeed, the flow visualization obtained by releasing smoke near the apex shows this type of instability (Fig. 3). In addition, the azimuthal wave number was estimated from the phase angle between the signals from two hot-wire probes located at $y/s = 0.5$ and $z/s = 0.25$ and $y/s = 0.5$ and $z/s = 0.75$. With respect to the vortex axis, these locations are approximately 180 deg apart. The probes were oriented so as to be most sensitive to tangential and axial velocities. The phase angle is shown in Fig. 4 for several values of angle of attack, which suggests that the azimuthal wave number is $n = 1$.

These results are consistent with the predictions of the linear stability theory.[8] Lessen et al. carried out their calculations for a jet-like axial velocity profile and showed that the flow is most sensitive to the disturbances with negative azimuthal wave numbers ($n < 0$). Translation and inversion of the axial velocity profile does not affect the growth rate within the temporal analysis. However, the azimuthal wave number changes its sign.[13] Therefore, for a wake-like profile such as found in breakdown region, the most unstable modes are the ones with positive azimuthal wave numbers ($n > 0$), which represent disturbances rotating in the same direction as the vortex. This is in agreement with the findings in Fig. 2. The theory cannot predict which azimuthal wave number will be amplified. However, experiments in a tube[4] and tip vortex[7] showed that $n = 1$. This is also in agreement with the present results (see Fig. 4). The $|n| = 1$ mode is necessary for a streakline released on the axis to take a helical shape,[4] since the radial velocity component must be zero on the axis for all modes except $|n| = 1$. In the breakdown region shown in Fig. 3, the large-scale helical shape of smoke, which is originated from the axis, is an evidence of the helical mode instability. Since the disturbances with $n = 1$ will have a phase function ($kx + \phi - \omega t$), one expects velocity/vorticity to be periodical in the x direction and be antisymmetric with

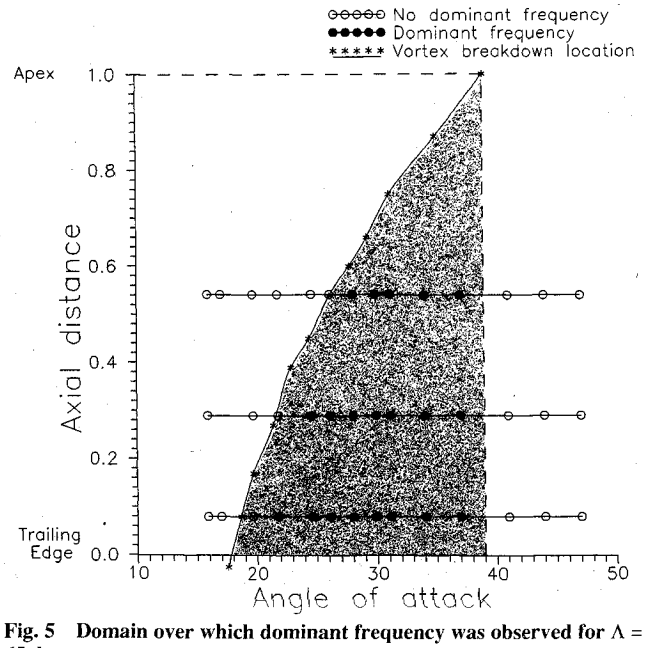

Fig. 5 Domain over which dominant frequency was observed for Λ = 65 deg.

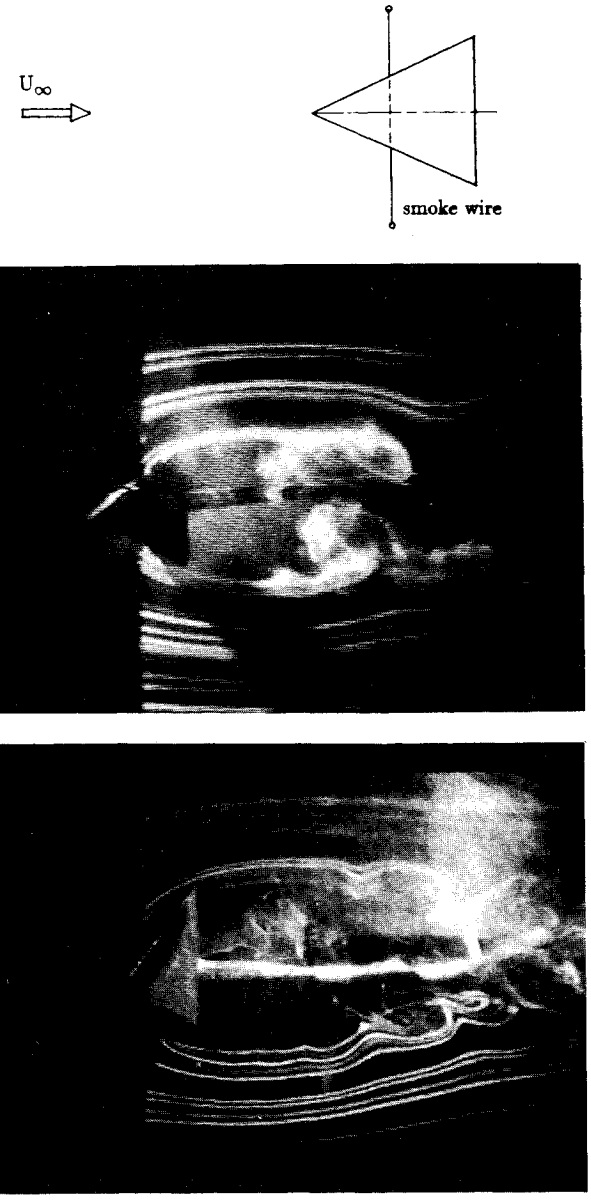

Fig. 6 Vortex shedding at large angle of attack (α = 60 deg), Λ = 60 deg and Λ = 75 deg, *Re* = 15,000.

respect to the vortex axis. Indeed, the instantaneous azimuthal vorticity in a plane through the vortex axis[14] shows that vorticity concentrations form the two rows of periodic structures located on either side of the axis with an antisymmetric configuration, resembling the well-known Karman vortex street.

With increasing angle of attack, the pressure spectra became free from any sharp peaks. The domain over which a sharp peak was observed in the spectrum for the wing with sweep angle Λ = 65 deg is shown in Fig. 5. A dominant frequency was observed at the measurement stations downstream of breakdown location, until the breakdown reached the apex of the wing. When the angle of attack is larger than the one that corresponds to the breakdown location at apex, no oscillations were observed in pressure fluctuations. The measurements for other wings gave results similar to Fig. 5. Thus, it is concluded that, until the breakdown reaches the apex of the wing, swirling flow persists over the wing and hydrodynamic instability of this flow is the only source of the unsteady loading on the wing. For larger angles of attack, the shear layer separated from the leading edge will not be able to form a swirling flow with axial motion. Thus, at large angle of attack, the vortex shedding from the wing starts as shown in Fig. 6. Whereas the shedding seems symmetric for the large aspect ratio wing, alternate shedding becomes dominant for the low aspect ratio wing. A

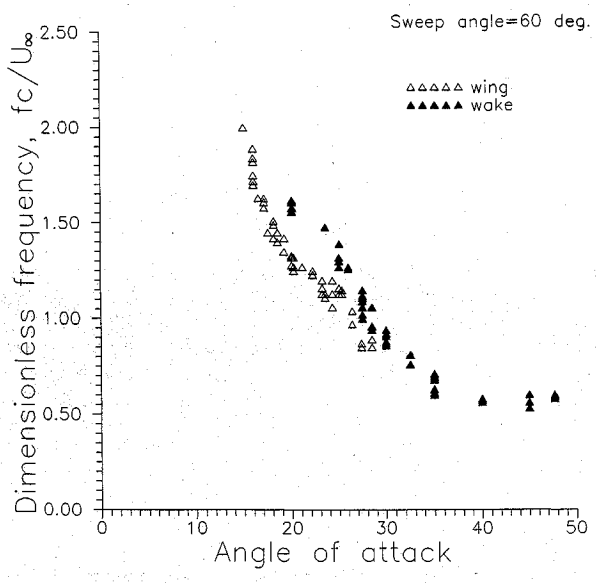

Fig. 7 Variation of dimensionless dominant frequency on the wing (x/c = 0.89) and at one chord length downstream of trailing edge as a function of angle of attack, Λ = 60 deg.

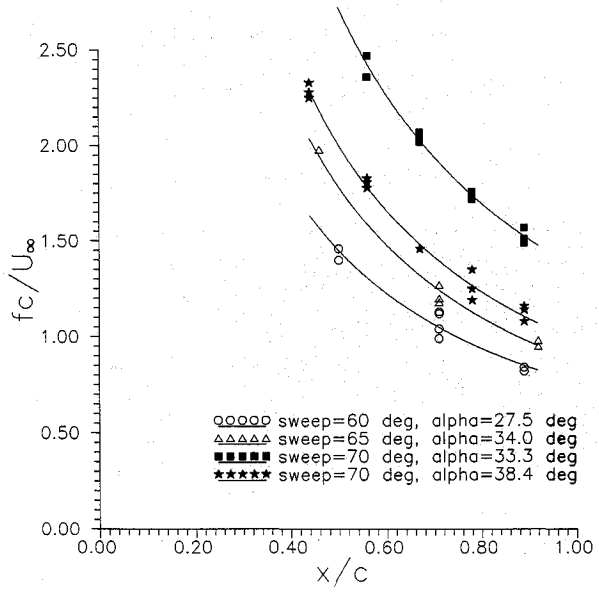

Fig. 8 Variation of dimensionless frequency fc/U_∞ as a function of streamwise distance.

signal from a hot-wire probe located at one chord length from the trailing edge was used to monitor unsteady flow in the wake. Dominant frequency detected in the wake was compared with the dominant frequency detected by the pressure transducer located near the trailing edge (x/c = 0.89) in Fig. 7. Until the breakdown location reaches the apex ($\alpha \simeq$ 30 deg for the wing with sweep angle Λ = 60 deg), both signals have the dominant frequency of the helical mode instability, although the frequencies differ slightly. This may be due to the streamwise gradients of the mean flow in the wake. Since no coherent pressure oscillations on the wing due to vortex shedding was detected (see also Fig. 5), this suggests that unsteady loading on the wing due to vortex shedding is negligible. After the helical mode instability disappears, vortex shedding frequency is detected in the wake. Although the relationship between the dominant frequency in the wake and angle of attack seems a continuous curve, it covers two different flow regimes. Indeed, in the vortex shedding regime, the frequency is pretty much constant. Similar trend was observed for a wing with Λ = 76 deg in other experiments.[9]

Measurements of pressure at different streamwise locations on the wing upper surface showed that the dominant frequency is not constant, but depends on the distance from the apex. Examples of variation of dimensionless frequency fc/U_∞ as a function of the streamwise distance for different wings is shown in Fig. 8. The scatter in the data is believed to be due to fluctuations in the breakdown location. It is well known that vortex breakdown location exhibits irregular variations. The dominant frequency decreases with increasing distance. This was also noticed by Roos and Kegelman[3] (for a wing with Λ = 70 deg and α = 33 deg); moreover, it was shown that if the frequency is normalized with the distance x, the dimensionless frequency fx/U_∞ is nearly constant. This was attributed to disturbances rotating in the vortex core whose radius grows linearly with x. The variation of fx/U_∞ corresponding to the data in Fig. 8 is shown in Fig. 9. It seems that fx/U_∞ is nearly constant for a given Λ and α for all delta wings tested. Since the disturbances are shown to be helical waves, this implies that the wavelength increases with x. Indeed, the instantaneous azimuthal vorticity in a plane through the vortex axis, which was recently obtained by a particle image velocimetry technique,[14] clearly shows vorticity concentrations with increasing wavelength between them. The instantaneous azimuthal vorticity concentrations seem to be located

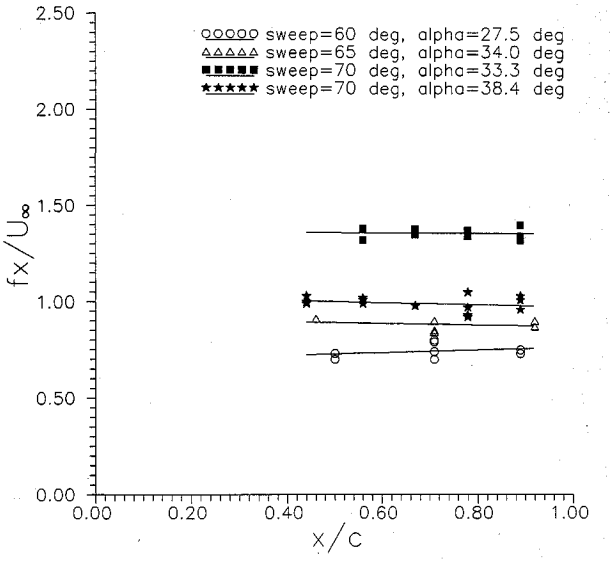

Fig. 9 Variation of dimensionless frequency fx/U_∞ as a function of streamwise distance.

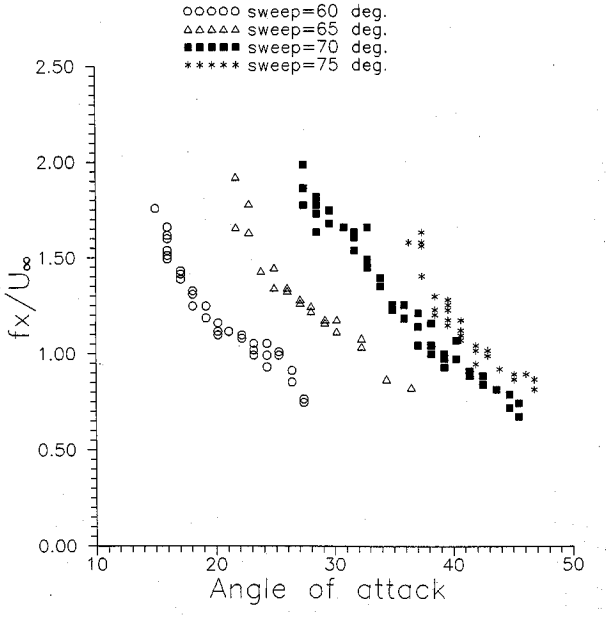

Fig. 10 Variation of dimensionless frequency fx/U_∞ as a function of angle of attack for different values of sweep angle.

on a cone. Moreover, the time-averaged velocity profile in the breakdown region was shown to be a function of r/x, indicating that the mean flow is conical.[3] Thus, the wavelength of the disturbance is expected to increase linearly with x in a conical mean flowfield.

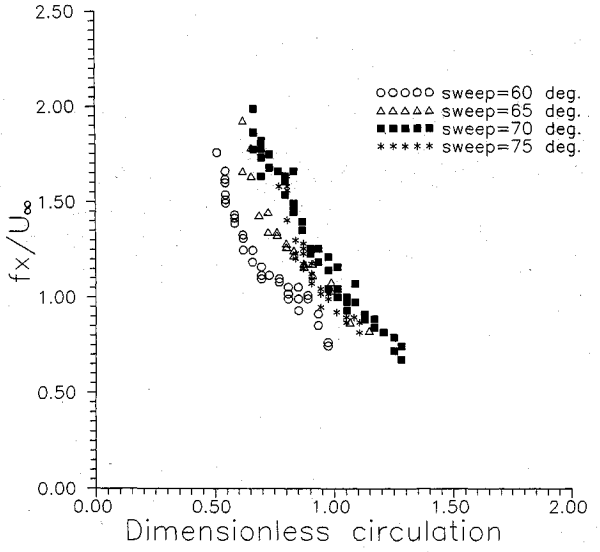

Fig. 11 Variation of dimensionless frequency fx/U_∞ as a function of dimensionless circulation $\Gamma/U_\infty x$.

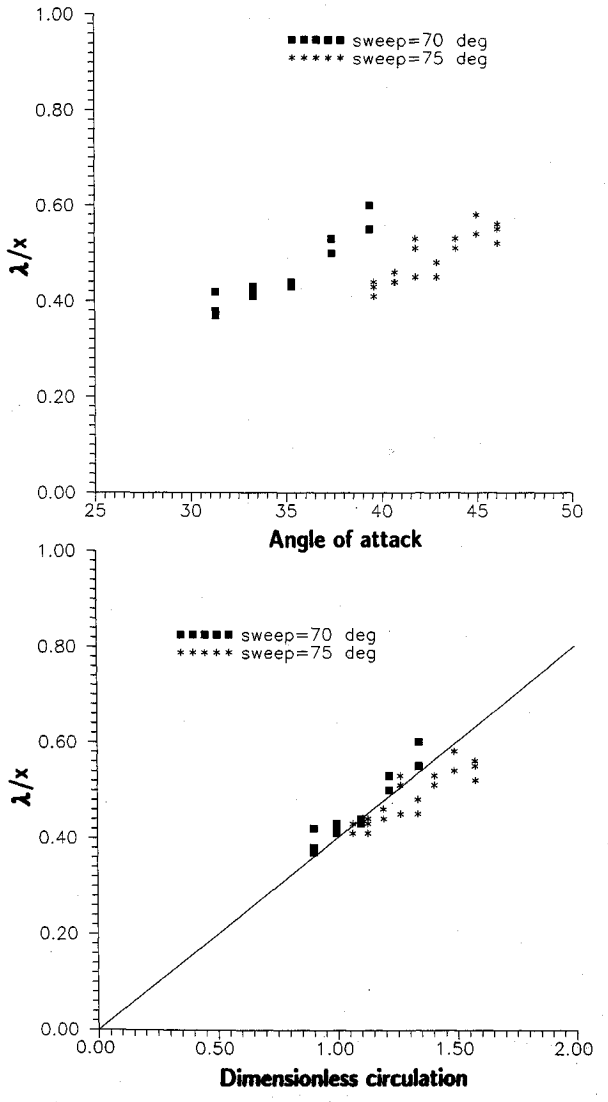

Fig. 12 Variation of normalized wavelength λ/x as a function of angle of attack (top) and dimensionless circulation (bottom), $x/c = 0.85$.

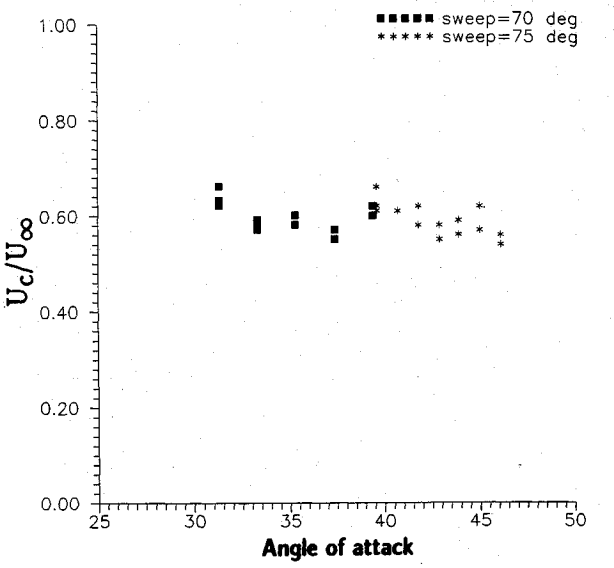

Fig. 13 Variation of phase speed as a function of angle of attack.

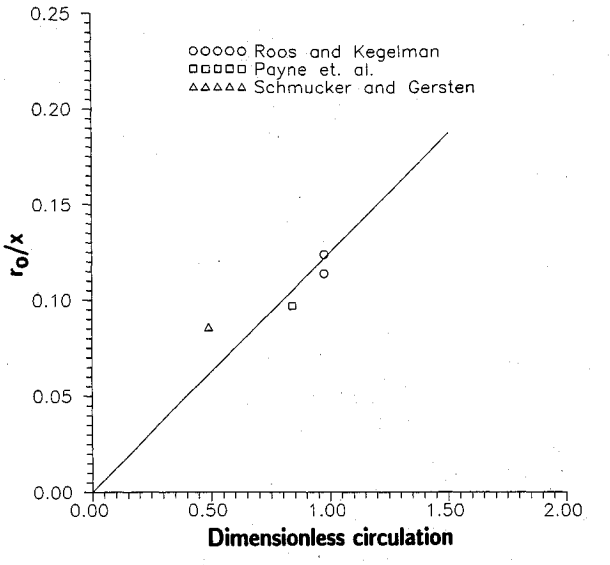

Fig. 14 Variation of normalized core radius r_0/x as a function of dimensionless circulation.

Having verified that fx/U_∞ is nearly constant for a given geometry (angle of attack and sweep angle), the variation of the dimensionless frequency is shown in Fig. 10 as a function of angle of attack for the four wings tested. The range of the data is nearly the same for different wings. This suggests that a single relationship can be obtained if a unique parameter is found. The circulation of the leading-edge vortex is considered, which depends on both angle of attack α and sweep angle Λ. Experiments on vortex breakdown over delta wings in steady[3] and unsteady freestream,[15] as well as on trailing vortices,[16] showed that the overall circulation is affected only very slightly after burst, although the vorticity concentration changes dramatically. Thus, it is reasonable to assume that the circulation continues to grow linearly, even after breakdown, because of continuous feeding of vorticity from leading edge. The dimensional analysis for the four variables Γ, U_∞, f, and x shows that two nondimensional numbers can be found and a single relationship exists,

$$\frac{fx}{U_\infty} = F\left(\frac{\Gamma}{U_\infty x}\right) \tag{1}$$

Since the circulation grows linearly with x, the dimensionless number $\Gamma/U_\infty x$ does not depend on x. The circulation for a given

angle of attack and sweep angle was estimated by using a slender wing theory.[17] Figure 11 shows that all of the curves collapse except for $\Lambda = 60$ deg. Since the method used to calculate circulation is a good approximation for low aspect ratio wings, the discrepancy for $\Lambda = 60$ deg is believed to be due to the incapability of the method to estimate the circulation.

The wavelength of the disturbance was measured by two pressure transducers located in the streamwise direction. From the phase measurements obtained by the cross-spectral analysis, the wavelength was calculated as $\lambda = 2\pi/(\partial\Phi/\partial x)$, where Φ is measured in radians. Typical distance between the transducers was $\Delta x/c = 0.066$, corresponding to $\Delta x/\lambda \simeq 0.13$. The midpoint between the transducers was located near the trailing edge ($x/c = 0.85$). Based on the previous results, the wavelength is expected to be linearly changing with x in the conical mean flowfield. The variation of λ/x as a function of angle of attack and dimensionless circulation is shown in Fig. 12. In addition, the variation of the phase speed $U_c = f\lambda$ is shown in Fig. 13. The quantity λ/x seems to be a linear function of the dimensionless circulation. A linear curve fit provided the following relation:

$$\frac{\lambda}{x} = 0.4\frac{\Gamma}{U_\infty x} \tag{2}$$

Since the normalized convection speed U_c/U_∞ seems to be independent of the dimensionless circulation, it can be shown that

$$\frac{\lambda}{x} = \frac{U_c}{fx} \sim \frac{U_\infty}{fx} = \frac{1}{(fx/U_\infty)}$$

and using Eq. (2)

$$\frac{\lambda}{x} \sim \frac{1}{(fx/U_\infty)} \sim \frac{\Gamma}{U_\infty x}$$

Hence,

$$\frac{fx}{U_\infty} \sim \left(\frac{\Gamma}{U_\infty x}\right)^{-1} \tag{3}$$

Indeed, a curve fit to the data shown in Fig. 11 gives the following relationship:

$$\frac{fx}{U_\infty} = 1.038\left(\frac{\Gamma}{U_\infty x}\right)^{-0.98}$$

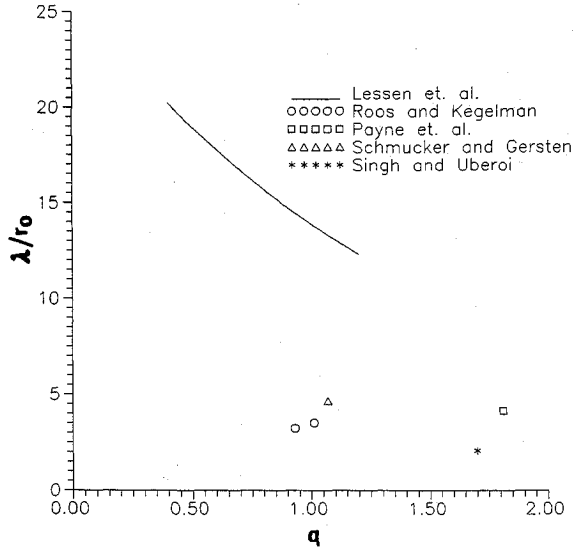

Fig. 15 Variation of λ/r_0 as a function of parameter q.

Lessen et al.[8] calculated the most unstable wavelength for the first helical mode of the following time-averaged mean flow:

$$V/U_s = \frac{q}{r/r_0}[1 - \exp(-r^2/r_0^2)]$$

$$W/U_s = \exp(-r^2/r_0^2) \tag{4}$$

where the circulation is $\Gamma = 2\pi q r_0 U_s$. This is known as Q vortex and the parameter q is directly proportional to the circulation and inversely proportional to the axial velocity excess or deficit U_s. The maximum swirl speed occurs at $r = 1.122\ r_0$. Therefore, the parameter r_0 can be taken as the characteristic core size. The most unstable wavelength λ/r_0 for the first helical mode was calculated by Lessen et al.[8] for several values of the parameter q. The core radius r_0 is expected to be a linear function of x in the conical flow over delta wings. From a limited number of mean velocity measurements,[3,18,19] r_0/x was estimated and is shown in Fig. 14. The data suggests that the core radius increases with the increasing swirl level, which was predicted for a trailing vortex[20] and swirling flows in tubes.[21] Although the data is very limited, there is a trend of a linear relationship between r_0/x and $\Gamma/U_\infty x$. This together with Eq. (2) suggests that the normalized wavelength λ/r_0 is roughly constant as is expected in a conical flowfield. The variation of λ/r_0 with the estimated parameter q is shown in Fig. 15, which indicates that the disturbances have a much smaller wavelength than the predictions for the Q vortex. This may be due to slowly varying mean flow in the streamwise direction. Garg and Leibovich[4] showed that the measured frequencies in vortex-tube experiments agree very well with the temporal stability predictions for the Q vortex, assuming that the disturbances have the wavelength and phase speed corresponding to the maximum growth rate. On the other hand, the experimental result for a trailing vortex[7] (for which the streamwise gradient is also negligible) is closer to the results for leading-edge vortex over delta wings. The discrepancy between the predictions for Q vortex and the present experimental results remains to be explained.

Conclusions

Experiments showed that coherent pressure fluctuations are observed on delta wings as long as vortex breakdown is over the wing. Cross-spectral analysis of two-point pressure and velocity measurements as well as flow visualization confirm that these oscillations are in the form of helical waves with azimuthal wave number $n = 1$, which is the result of the instability of swirling breakdown wake flow. The source of unsteady loading on the wing is due to this helical mode instability as opposed to vortex shedding which starts after the breakdown reaches the apex of the wing. Vortex shedding takes the form of symmetric or alternate depending on the aspect ratio of the wing. The influence of vortex shedding on unsteady pressure fluctuations is negligible and could not be detected in the experiments, although the velocity fluctuations in the wake show coherent oscillations.

Measurements of unsteady pressure at different streamwise locations on the wing surface showed that the dimensionless frequency fx/U_∞ is nearly constant for a fixed angle of attack and sweep angle. Based on the results from this work and other experiments, it is suggested that the wavelength of the disturbances increases linearly with x in the conical mean flowfield, resulting in constant fx/U_∞. The nondimensional frequency is found to be a function of nondimensional circulation $\Gamma/U_\infty x$ only, where the circulation was calculated by assuming conical flow and using a slender-wing theory.

Measurements of the wavelength and phase speed indicates that λ/x increases with increasing $\Gamma/U_\infty x$, whereas the phase speed is roughly constant $U_c/U_\infty \simeq 0.6$. The core radius r_0 which is approximately equal to the radius at which the swirl speed becomes maximum, also increases with increasing $\Gamma/U_\infty x$. The normalized wavelength λ/r_0 seems to be around 3–4, which is much smaller than the predictions for the Q vortex.

Finally, it should be noted that the existence of helical mode instability does not have any implications with regard to the breakdown mechanism. The flows upstream of breakdown location are known to be stable to disturbances. However, whether the instabilities in downstream region promote breakdown is not known.[4]

Acknowledgments

Part of this work was supported by the Air Force Office of Scientific Research. The author would like to thank F. Roos for making some of his data available.

References

[1]Earnshaw, P. B., and Lawford, J. A., "Low Speed Wind Tunnel Experiments on a Series of Sharp-edged Delta Wings," Aeronautical Research Council, R & M 3424, Aug. 1964.

[2]Mabey, D. B., "Beyond the Buffet Boundary," *Aeronautical Journal,* April 1973, pp. 201–215.

[3]Roos, F. W., and Kegelman, J. T., "Recent Explorations of Leading-edge Vortex Flowfields," NASA High-Angle-of-Attack Technology Conference, NASA Langley Research Center, Hampton, VA, Oct. 30–Nov. 1, 1990.

[4]Garg, A. K., and Leibovich, S., "Spectral Characteristics of Vortex Breakdown Flowfields," *Physics of Fluids,* Vol. 22, No. 11, 1979, pp. 2053–2064.

[5]Chanaud, R. C., "Observations of Oscillatory Motion in Certain Swirling Flows," *Journal of Fluid Mechanics,* Vol. 21, 1965, pp. 111–127.

[6]Cassidy, J. J., and Falvey, H. T., "Observations of Unsteady Flow Arising after Vortex Breakdown," *Journal of Fluid Mechanics,* Vol. 41, 1970, pp. 727–736.

[7]Singh, P. I., and Uberoi, M. S., "Experiments on Vortex Stability," *Physics of Fluids,* Vol. 19, No. 12, 1976, pp. 1858–1863.

[8]Lessen, M., Singh, P. J., and Paillet, F., "The Stability of a Trailing Line Vortex, Part 1, Inviscid Theory," *Journal of Fluid Mechanics,* Vol. 63, 1974, pp. 753–763.

[9]Rediniotis, O. K., Stapountzis, H., and Telionis, D. P., "Vortex Shedding over Delta Wings," *AIAA Journal,* Vol. 28, No. 5, 1990, pp. 944–946.

[10]Wentz, W. H., and Kohlman, D. L., "Vortex Breakdown on Slender Sharp-Edged Wings," *Journal of Aircraft,* Vol. 8, No. 2, 1971, pp. 156–161.

[11]Erickson, G. E., "Water-Tunnel Studies of Leading-Edge Vortices," *Journal of Aircraft,* Vol. 19, No. 3, 1982, pp. 442–448.

[12]Hummel, D., "Untersuchungen uber das Aufplatzen der Wirbel an schlanken Deltaflugeln," *Zeitschrift fuer Flugwissenshaft,* Vol. 13, 1965, pp. 158–168.

[13]Khorrami, M., "On the Viscous Modes of Instability of a Trailing Line Vortex," *Journal of Fluid Mechanics,* Vol. 225, 1991, pp. 197–212.

[14]Rockwell, D., Magness, C., Robinson, O., Towfighi, J., Akin, O., Gu, W., and Corcoran, T., "Instantaneous Structure of Unsteady Separated Flows via Particle Image Velocimetry," Fluid Mechanics Labs., Lehigh Univ., Rept. PI-1, Bethlehem, PA, Feb. 1992.

[15]Gursul, I., and Ho, C. M., "Vortex Breakdown over Delta Wings in Unsteady Free Stream," AIAA Paper 93-0555, Jan. 1993.

[16]Solignac, J. L., and Leuchter, O., "Etudes experimentales d'ecoulements tourbillonaires soumis a des effets de gradient de pression adverse," *Aerodynamics of Vortical Type Flows in Three Dimensions,* AGARD CP-342, July 1983.

[17]Smith, J. H. B., "Improved Calculations of Leading-Edge Separation from Slender, Thin, Delta Wings," *Proceedings of the Royal Society, A,* Vol. 306, 1968, pp. 67–90.

[18]Payne, F. M., Ng, T. T., Nelson, R. C., and Schiff, L. B., "Visualization and Wake Surveys of Vortical Flow over a Delta Wing," *AIAA Journal,* Vol. 26, No. 2, 1988, pp. 137–143.

[19]Schmucker, A., and Gersten, K., "Vortex Breakdown and its Control on Delta Wings," *Fluid Dynamics Research,* Vol. 3, 1988, pp. 268–272.

[20]Mager, A., "Dissipation and Breakdown of a Wing-Tip Vortex," *Journal of Fluid Mechanics,* Vol. 55, 1972, pp. 609–628.

[21]Keller, J. J., Egli, W., and Althaus, R., "Vortex Breakdown as a Fundamental Element of Vortex Dynamics," *Fluid Dynamics Research,* Vol. 3, 1988, pp. 31–42.